Sustainable Materials and Technologies 38 (2023) e00765

Contents lists available at ScienceDirect

Sustainable Materials and Technologies

journal homepage: www.elsevier.com/locate/susmat

Waste printer ink as modifier for natural rubber/carbon black composites: No haste, use waste

Aleksander Hejna [a,*], Paulina Wiśniewska [b], Daria Kowalkowska-Zedler [c], Jerzy Korol [d], Paulina Kosmela [b], Mariusz Marć [e], Peyman Ezzati [f], Marek Szostak [a], Mohammad Reza Saeb [g,*]

[a] Institute of Materials Technology, Poznan University of Technology, Piotrowo 3, Poznań 60-965, Poland
[b] Department of Polymer Technology, Gdańsk University of Technology, Narutowicza 11/12, Gdańsk 80-233, Poland
[c] Department of Inorganic Chemistry, Gdańsk University of Technology, Narutowicza 11/12, Gdańsk 80-233, Poland
[d] Department of Mechanical Testing and Material Engineering, Central Mining Institute, Plac Gwarków 1, Katowice 40-166, Poland
[e] Department of Analytical Chemistry, Gdańsk University of Technology, Narutowicza 11/12, Gdańsk 80-233, Poland
[f] ERA Co., Ltd, Science and Technology Center, P.O. Box: 318020, Taizhou, Zhejiang, China
[g] Department of Pharmaceutical Chemistry, Medical University of Gdańsk, J. Hallera 107, 80-416 Gdańsk, Poland

ARTICLE INFO

Keywords:
Waste management
Natural rubber
Carbon black
Surface area
Volatile organic compounds emission

ABSTRACT

From a sustainability perspective, achieving a greener future with a minimal carbon footprint requires maximizing waste materials' reuse. Typically, processing, price, properties, and performance are the four pillars of satisfying customer demands. Armed with this vision, the present work seeks to utilize waste printer ink (WPI) as a source of carbon in combination with low- and high-surface carbon black (LCB and HCB, respectively) additives to enhance the properties and performance of natural rubber (NR). Using WPI-modified CB together with NR underlines the importance of this work from a sustainability angle. By altering the type and amount of CB and WPI content, a broad properties window was unraveled, such that a very high elongation at break of ~970% and elasticity of 53% were achieved under optimized conditions and formulation, when compared with 385% and 27.5% values of the reference blank NR sample, respectively. Thermal stability was also changed quite broadly, depending on the formulation. The analysis of volatile organic compounds (VOCs) revealed that propanol and its derivatives were the most abundant volatiles detected, accounting for more than 85% of the total emission. Analyzing environmental contamination and properties investigations opened avenues to propose practical ideas and strategies in order to standardize the usage of WPI and CB additives in NR compounding.

1. Introduction

Polymer composites and nanocomposites combine the advantages of polymers, such as the outstanding resistance to chemicals, lightness, and flexibility to the processing with the promising characteristics of organic and/or mineral filler/additives in order to achieve a higher thermal [1], mechanical [2] flame retardant [3], and electrical properties and performance [4,5], particularly compared to their metal counterparts. Rubber composites are a foremost class of polymer composites widely studied and manufactured for myriad applications ranging from bitumen and end-of-life tire recycling to medical devices and systems [6,7]. In this regard, a quite wide variety of fillers and additives ranging from bio-waste [8] and mineral [9] to carbonaceous fillers such as carbon nanotubes (CNTs) [10], graphite and graphene [11], have been examined in rubbers from simple to complex hybrid systems [12]. Overall, the degree of success in achieving a high-performance rubber composite severely depends on the degree of interfacial adhesion between the rubber matrix and additives, which necessitae precise design and formulation, along with implementation of efficient processing methods [13,14].

Due to their extraordinary features, such as electrical and thermal conductivity, charring behavior, and anti-corrosive properties, carbonaceous fillers have frequently been considered as the first candidates for developing high-performance rubber composites [15]. On the other hand, environment protection and safety regulations have additionally stressed the consideration of two more vital aspects in the design, formulation, and manufacture of rubber composites, i.e., prioritizing wasted and recycled fillers/additives and the use of commercially

* Corresponding authors.
E-mail addresses: aleksander.hejna@put.poznan.pl (A. Hejna), mrsaeb2008@gmail.com (M.R. Saeb).

https://doi.org/10.1016/j.susmat.2023.e00765
Received 28 September 2023; Accepted 1 November 2023
Available online 4 November 2023

available carbon-based fillers [16–18]. There is no denying that carbon black (CB) should be the first additive to be prioritized among carbonaceous fillers considered for developing rubber composites, given its mechanical properties and crosslinking privileges, particularly towards natural rubber (NR) [19]. Typically, increasing the amount of CB leads to the morphological transition from amorphous into semi-crystalline structures, which substantially affects the ultimate properties of NR composites. Nevertheless, CB has been known to be the most reliable carbonaceous filler for NR, given its anisotropic features, which govern the mechanical reinforcement mechanism [20].

There are several parameters, such as the surface chemistry and morphology of CB, along with modification of the NR matrix, which interrelatedly affect the ultimate performance of NR composites [21,22]. Among elaborated investigations, the one performed by Salaeh and Nakason contained several sorts of NR composites by comparing unmodified, epoxidized, and maleated NR together with variation of the type of CB providing different surface area and morphology [23]. They reported that the degree of crosslinking and electrical conductivity of NR composites have markedly changed, as a result of the change in the degree of physical and chemical interactions, contributed from the surface area and presence of polar functional groups on the surface of CB. A more sustainable approach was presented elsewhere by replacing and/or modifying CB in NR composites [24,25]. Very recently, the recycling and reuse of waste printer inks (WPI) [26,27] and printer toner [28] have become more and more attuned to the needs of sustainability, but yet no systematic report was published on WPI incorporation into rubbers.

In light of the above, we hypothesized that WPI, because of being liquid and resembling oil from one side and being rich in carbon from the other side, could have been a potential modifier for developing partially sustainable high-performance NR/CB rubber composites, which has not been reported yet. In this work, NR composites comprising two types of CB with low and high surface area (hereafter referred to as LCB and HCB, respectively) along with WPI were formulated and underwent complete characterization, including volatile organic compounds (VOCs) emission, swelling behavior (crosslink density evaluation), rheological behavior (curing characteristics), thermal stability with thermogravimetric analysis (TGA), abrasion, rebound resilience, sol fraction, thermal behavior (differential scanning calorimetry – DSC), tensile performance and dynamic mechanical analysis (DMA). Attention was paid to exploring the correlation between curing and thermo-mechanical properties, highlighting the role of WPI as a prominent modifier of NR/CB composites. Moreover, properties were interpreted based on the molecular interaction between the filler and rubber matrix, where surface chemistry and specific surface area could play the main roles.

2. Experimental

2.1. Materials

Two types of carbon black (CB) were applied in the presented study. The first type was Chezacarb AC-60 (HCB) acquired from ORLEN Unipetrol a.s. (Czech Republic) and characterized by the iodine value >950 $g \bullet kg^{-1}$, oil absorption number > 380 $cm^3 \bullet 100\ g^{-1}$, sieve residue at 45 μm <0.05 wt%, bulk density > 112 $kg \bullet m^{-3}$, and nitrogen surface area > 800 $m^2 \bullet g^{-1}$. The second one was Carbon Black PP 1201 PB (LCB) obtained from Phillips Carbon Black Limited (India) and characterized by the iodine value of 127 $g \bullet kg^{-1}$, oil absorption number of 114 $cm^3 \bullet 100\ g^{-1}$, sieve residue at 45 μm equal to 0.0011 wt%, bulk density of 342 $kg \bullet m^{-3}$, and nitrogen surface area of 192 $m^2 \bullet g^{-1}$. Comparatively, HCB shows a noticeably higher specific surface area, which can be attributed to the reduced density.

Waste printer ink (WPI) has been applied as a modifier of CB. They were obtained from the local recycling company (Katowice, Poland) and, according to the company, contained pigments, resins, and organic solvents, mainly ethanol, ethyl acetate, n-propanol, ethoxypropanol, methoxypropanol, and *n*-propyl acetate.

Natural rubber (NR) obtained from Guma-Pomorska (Poland) as ribbed smoked sheets with a density of 0.92 $g \bullet cm^{-3}$ were applied as the matrix for prepared composites. It was used as received without additional modifications.

Stearic acid (SA) obtained from Standard Sp. z o.o. (Poland) was applied as a plasticizer and activator of vulcanization during composites' preparation. It was characterized by a density of 0.94 $g \bullet cm^{-3}$ and a melting temperature of 69.3 °C.

Zinc oxide (ZO) acquired from Standard Sp. z o.o. (Poland) was applied as an activator of vulcanization. It was characterized by a density of 5.61 $g \bullet cm^{-3}$.

N-tert-butyl-2-benzothiazole sulfonamide (TBBS) and 2-mercaptobenzothiazole (MBT) were used as vulcanization accelerators. They were obtained from Standard Sp. z o.o. (Poland) and characterized by the density of 1.29 and 1.54 $g \bullet cm^{-3}$, respectively, and the melting temperature of 104–111 and 173 °C, respectively.

Sulfur (S) acquired from Standard Sp. z o.o. (Poland) was used as a vulcanization agent. It was characterized by a density of 2.07 $g \bullet cm^{-3}$ and a melting temperature of 115 °C.

2.2. Modification of CB with WPI

Two types of CB were mixed with the WPI using the Intensive Mixer Eirich R02 manufactured by Maschinenfabrik Gustav Eirich (Germany). The mixer was equipped with a star-belt type stirrer rotating opposite to the mixer pan rotation. Intensive mixers enable the efficient mixing of components because around 90% of energy would be compensated for the mixing. Therefore, a high degree of homogeneity could principally and relatively quickly be achieved. Moreover, the intensive mixers could allow the simultaneous mixing and granulation of the material, enabling the disintegration and fragmentation of agglomerates. The following process parameters were used: agitator rotations at 1700 rpm, pan rotations at 60 rpm, and mixing time of 30 s.

The compositions were based on the maximum content of CB possible to introduce into the WPI. For HCB, it was 80 parts by weight, while for LCB, 100 parts by weight per 100 parts of WPI. Such a difference was fuelled by the difference between specific surface areas of particular CB samples. Therefore, samples $HCB_{0.4}$ and $HCB_{0.8}$ contained 40 and 80 pbw of HCB for 100 pbw of WPI, respectively, while samples $LCB_{0.5}$ and $LCB_{1.0}$ contained 50 and 100 pbw of LCB for 100 pbw of WPI, respectively.

2.3. Preparation of NR/CB rubber composites

As-received and modified CB samples were mixed with NR at ambient temperature using a two-roll mill model 14,201/P2 from Buzuluk (Czech Republic). Formulations of samples are presented in Table 1. Mixing included a 2-min mastication of NR, then ZO and SA were added. Fillers were introduced after 4 mins, TBBS and MBT after 12 mins, and S after 15 min. Mixing time equaled 17 min. The obtained composites were compression molded at 160 °C and 4.9 MPa according to the determined optimal cure time.

2.4. Characterization techniques

Volatile matter content in as-received and modified CB samples was determined using a moisture analyzer MA 50/1.X2.IC.A.WH from Radwag Wagi Elektroniczne (Poland). Samples weighing approximately 1 g were analyzed at temperatures from 60 to 150 °C (in 10 °C intervals) until mass change was lower than 1 mg/min.

To indirectly assess the adsorption capacity of the samples, they were placed in different solvents for 72 h. Solvents, acetone, methanol, and toluene, have been selected based on the different values of the polarity index, equaling 0.355, 0.762, and 0.099, respectively, according to

Table 1
Formulations of the prepared NR-based composites containing modified CBs, along with the reference sample – unfilled vulcanized NR.

Component	Content, parts by weight						
	R0	RHCB	RLCB	$RHCB_{0.4}$	$RHCB_{0.8}$	$RLCB_{0.5}$	$RLCB_{1.0}$
NR	100	100	100	100	100	100	100
Curing system*	6.2	6.2	6.2	6.2	6.2	6.2	6.2
HCB		30					
LCB			30				
$HCB_{0.4}$				30			
$HCB_{0.8}$					30		
$LCB_{0.5}$						30	
$LCB_{1.0}$							30
CB content, phr	0	30.0	30.0	8.6	13.3	10.0	15.0
CB content, %	0	22.0	22.0	6.3	9.8	7.3	11.0

* Curing system composition: ZO – 2.5 phr, SA – 0.3 phr, TBBS – 0.7 phr, MBT – 0.7 phr, S – 2.0 phr.

Reichardt [29]. After 72 h, the samples were photographed.

The organic compounds emission investigations were performed using stationary emission chambers system (Micro-Chamber/Thermal Extractor™ (μ-CTE™ 250, Markes International, Inc.) which contains four equal chambers made of polished stainless steel (internal volume of a single chamber - 114 cm^3) [30,31]. Before analysis, CB samples were placed on Petri dishes and weighed (average weight of analyzed samples – 0.200 ± 0.010 g). After this, 2 μL of deuterated toluene (Toluene-d_8 solution certified reference material containing 2000 μg·mL of Toluene-d_8 in 1 mL of MeOH, TraceCERT®, Merck, KGaA, Darmstadt, Germany) was injected on each of investigated sample as an internal standard (to assess the total VOCs (TVOCs), which were emitted to the gaseous phase). Next, CB samples were installed inside a chamber, sealed, and conditioned under the following conditions: inert gas (nitrogen; RH = 0%) flow rate – 12 $mL{\cdot}min^{-1}$; temperature – 30 °C; conditioning time – 10 min. Emitted from the CB samples, organic compounds were collected on stainless steel tubes filled with Tenax TA (60/80 mesh, stainless steel TD tube, O. D. × L 1/4 in. × 3 1/2 in., preconditioned, Merck KGaA, Darmstadt, Germany). After this, adsorbed on the surface of Tenax TA organic compounds were liberated using two-stage thermal desorption technique (TD) under following conditions: (i) Tenax TA tube desorption temperature – 285 °C; 1st stage desorption time - 10 min; gas flow rate (helium) – 50 $mL{\cdot}min^{-1}$; focusing cold trap temperature – 0 °C; (ii) focusing cold trap desorption temperature (ballistic heating) – 300 °C; 2nd stage desorption time – 5 min; gas flow rate (helium) – 2 $mL{\cdot}min^{-1}$. The injection of liberated analytes from the cold trap to gas chromatography (GC) capillary column in a splitless (as-received CBs) as well as in a split mode (WPI-modified CBs) (split set on a cold trap) 1:12. The TVOC parameter assessment was performed according to general procedure [32] using TD (Markes Series 2 Thermal Desorption Systems; UNITY/TD-100 (Markes International, Inc.) combined with GC and flame ionization detector (Agilent Technologies 7820 A GC System). The final determination stage was carried out under the following GC-FID conditions: FID temperature – 280 °C; TD-GC transfer line temperature – 180 °C; GC capillary column (30 m × 320 μm × 5 μm, J&W DB-1, USA); helium (He, 5.0) constant flow rate - 2.0 $mL{\cdot}min^{-1}$; oven temperature program: 50 °C maintained for 1 min, next increased 7 $°C{\cdot}min^{-1}$ up to 180 °C and hold for 1 min, finally increased 20 $°C{\cdot}min^{-1}$ up to 260 °C and maintained for 5 min. For qualitative screening analysis of the VOCs that were emitted to the gaseous phase from investigated CB samples, the TD (Markes Unity v.2 (Markes International, Inc.) system combined with GC (Agilent Technologies 6890) mass spectrometry (5873 Network Mass Selective Detector, Agilent Technologies) was applied. The main thermal extraction and injection conditions were the same as in the TD system mentioned earlier. The working parameters of the GC–MS system were as follows: GC capillary column - 30 m × 250 μm × 1 μm (J&W HP-1MS, USA); MS ion source temperature – 250 °C; the quadrupole mass analyzer temperature – 150 °C; GC–MS transfer line temperature – 280 °C. The GC oven working conditions were the same as in the mentioned earlier GC-FID system. The screening identification of emitted organic compounds was performed using the mass spectra database (NIST 2.0 Mass Spectral Library) linked to the MS system software (The NIST Mass Spectral Search Program for the NIST/EPA/NIH Mass Spectral Library Version 2.0 d, USA).

The thermal stability of CB samples and resulting NR-based composites were assessed using a TG 209F3 thermal analyzer from Netzsch (Germany). Analyses were performed under an N_2 atmosphere, in the temperature range of 30–900 °C (heating rate of 10 $°C{\bullet}min^{-1}$), for ~10 mg samples.

Curing characteristics were investigated according to ISO 3417, using a Monsanto R100S rheometer with an oscillating rotor (USA). The cure rate index (CRI) was calculated according to Eq. (1):

$$CRI = 100/(t_{90} - t_1) \quad (1)$$

where: t_{90} – optimum vulcanization time, min; t_1 – scorch time, min.

The aging resistance at elevated temperatures was determined using an R_{300} parameter [33], which is the percentage reversion degree after a period of 300 s calculated from the time of reaching the maximum torque value. R_{300} was calculated according to Eq. (2):

$$R_{300} = (M_H - M_{300s})/M_H \times 100\% \quad (2)$$

where: M_H – maximum torque, dNm; M_{300s} – torque 300 s after maximum torque, dNm.

The Mooney viscosity (MV) of the rubber compounds was measured at 100 °C using a Mooney viscosimeter MV2000 from Alpha Technologies (USA) according to ISO 289-1.

Abrasion resistance was measured using an abrasion tester from Gibitre Instruments (Italy) according to the standard ISO 4649. The abrasion resistance value averages at least three measurements per sample.

The rebound resilience was determined with a Schob-type pendulum Zwick 5109 (Germany). The analysis was performed following the ISO 4662 standard. Each evaluation was prepared for 7 test specimens.

The swelling degree of the blends (approx. 0.2 g samples) as a function of time was determined by equilibrium swelling in toluene (at room temperature). The swelling degree was calculated according to Eq. (3):

$$Q = (m_t - m_0)/m_0 \times 100\% \quad (3)$$

where: Q – swelling degree, %; m_t – a sample mass swelled after time t, g; m_0 – an initial mass of the sample, g.

The sol fraction was determined based on the mass difference between the initial sample and the dried sample after extraction according to Eq. (4). The remaining part is a gel fraction (5):

$$F_{sol} = (m_0 - m_k)/m_0 \times 100\% \quad (4)$$

$$F_{gel} = 100\% - F_{sol} \quad (5)$$

where: F_{sol} – the content of sol fraction, %; F_{gel} – the content of gel fraction, %; m_0 – an initial mass of the sample, g; and m_k – a mass of the dried sample after extraction, g.

Crosslink density was determined according to the Flory–Rehner Eq. (6) [34]:

$$\nu_x = \frac{-\left[ln(1-\phi_{gel}) + \phi_{gel} + \psi\phi_{gel}^2\right]}{\left[V_{solv}\left(\phi_{gel}^{1/3} - \frac{\phi_{gel}}{2}\right)\right]} \quad (6)$$

where: ν_x – crosslink density, mol•cm^{-3}; ϕ_{gel} – the volume content of gel fraction, %; ψ – polymer-solvent interaction parameter; V_{solv} – solvent

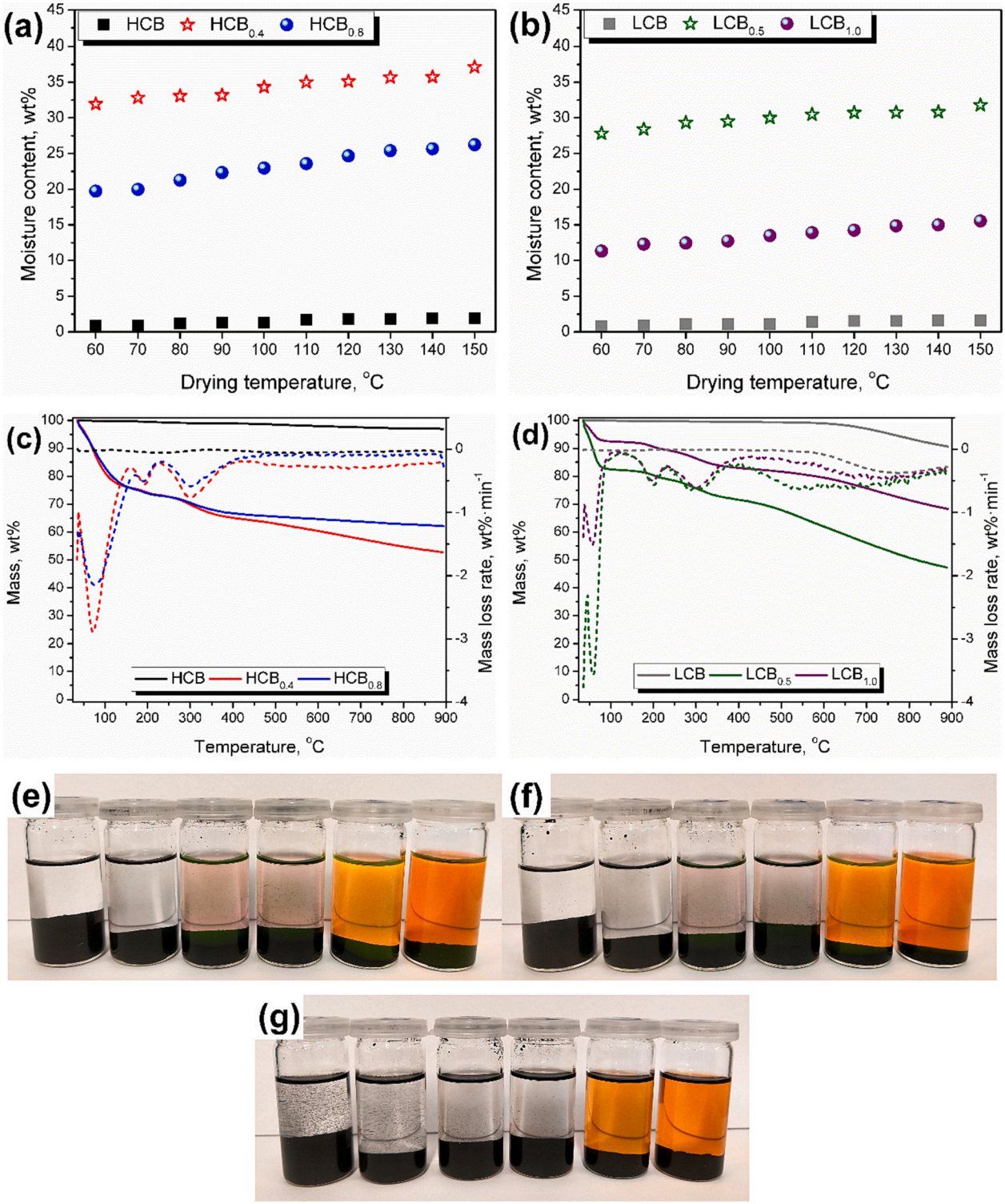

Fig. 1. The moisture content of as-received and modified CBs, (a) HCB and (b) LCB, at various temperatures, mass loss curves (straight lines), and differential thermogravimetric curves (dashed lines) for as-received and modified CBs, (c) HCB and (d) LCB, samples, and the appearance of the samples after 72-h immersion in: (e) acetone, (f) methanol, and (g) toluene. The order of samples (from left to the right): HCB, LCB, $HCB_{0.4}$, $HCB_{0.8}$, $LCB_{0.5}$, and $LCB_{1.0}$.

molar volume.

The Flory–Rehner equation is correct for non-filled compounds, which is not in line with the presence of high content of CB in the examined materials. Therefore, the Kraus correction should be included to calculate the actual crosslink density [35]. The correction was calculated following eqs. (7) and (8):

$$\nu_{x\ corrected} = \frac{\nu_x}{1 \bullet \Gamma \bullet \Xi} \tag{7}$$

$$\Xi = \frac{\Theta_{filler} \bullet \xi_{matrix} \bullet m_0}{\xi_{filler} \bullet m_k} \tag{8}$$

where: $\nu_{x\ corrected}$ – crosslink density after correction, mol•cm^{-3}; Γ – filler-characteristic constant (1.17 assuded in the presented work), solvent independent; Θ_{filler} – volume fraction of filler; ξ_{matrix} – matrix density, g•cm^{-3}; ξ_{filler} – filler density, g•cm^{-3}.

The density of prepared composites was determined using an Ultrapyc 5000 Foam gas pycnometer from Anton Paar (Austria). Following measurement settings were applied: gas – nitrogen; target pressure – 18.0 psi; flow direction – sample first; temperature control – on; target temperature – 20.0 °C; flow mode – monolith; cell size – small, 10 cm^3; preparation mode – flow; time of flow – 0.5 min.

Differential scanning calorimetry analysis was performed to analyze the thermal performance of prepared composites. Approximately 10 mg samples were placed in aluminum crucibles with pierced lids. They were heated from 20 to 200 °C with a heating rate of 10 °C•min^{-1}, then cooled to −80 °C with a cooling rate of 10 °C•min^{-1} and heated again to 200 °C with a heating rate of 10 °C•min^{-1}. The heating/cooling cycle was performed twice to erase the samples' thermal history during the first heating. The measurements were conducted in an inert N_2 atmosphere using a Netzsch 204F1 Phoenix apparatus (Germany).

The dynamic mechanical analysis was conducted on a DMA Q800 TA Instruments apparatus (USA). Samples with dimensions of 18 × 10 × 2 mm were loaded with variable sinusoidal deformation forces in the single cantilever bending mode at 1 Hz under the temperature rising rate of 4 °C•min^{-1}, ranging from −100 to 150 °C.

Strength properties were estimated by determining the tensile strength, elongation at break, and tear strength. The tests were carried out based on the PN-EN ISO 527 and ASTM D624 standards using the Instron 4465H 1937 testing machine (USA) with an elongation head and an extensometer. The elongation rate was 500 mm•min^{-1} to measure tensile strength and elongation at break and 50 mm•min^{-1} for tear strength. For each material, at least five samples were analyzed.

3. Results and discussion

3.1. Properties of modified CBs

Fig. 1 presents the moisture content of as-received and modified CB samples at particular temperatures determined by the moisture analyzed. It points to volatile matter content, the course of their thermal degradation, and their appearance after immersion in acetone, methanol, and toluene lasting 72 h. It can be seen that volatile content is at a similar level for both types of as-received CB, which was related to their similar chemical composition. Thermogravimetric curves confirmed these similarities. Values of thermal decomposition onset, determined as the temperature of 2 wt% mass loss, were 592.4 and 662.2 °C, while char residue equaled 96.92% and 90.58%, respectively, for HCB and LCB materials.

On the other hand, significant differences have been noted between modified HCB and LCB materials, pointing to the varying adsorption capacity due to the particle size and surface area differences. For HCB, the moisture content and the mass loss during the initial degradation phase (up to 200 °C) were noticeably higher than for LCB. Such an effect pointed to the higher amount of WPI adsorbed by HCB particles. Considering the shares of as-received CBs in modified samples, the adsorption capacity (calculated as a quotient of WPI share in moisture content and CB content of a particular sample) was twice as high for HCB.

The immersion tests have been conducted to assess the interfacial interactions between CBs and applied WPI indirectly. The appearance of samples after analysis points to the significant differences related to the HCB and LCB surface properties, confirming data provided by producers. For as-received CBs, solvents were transparent, pointing to the absence of extractives, which also aligns with the TGA analysis results.

However, for the samples soaked in toluene, suspended particles were noted contrary to acetone and methanol, which points to the relatively low polarity of CBs' surface, especially for HCB [36]. Modifying CB samples with WPI noticeably changed the results of the performed test. The color of the solvents changed after immersion, which points to the extraction of WPI components from modified CBs. For HCB, the most substantial effect was noted for acetone, which aligns with the polarity of solvents reported by the supplier as WPI components. For LCB, the effect appears to be similarly noticeable for all solvents. The differences between modified HCB and LCB samples confirm the differences in their surface properties and indicate significantly stronger interactions with WPI for HCB material, which can be attributed to the higher specific surface area. Observed differences may show the impact on the properties of polymer composites due to the potential migration of WPI from filler.

For a deeper understanding of the CBs' adsorption potential toward WPI and assessment of their environmental impact, the emissions of VOCs from modified HCB and LCB samples were analyzed. Fig. 2 provides insights into the total VOCs emissions (expressed by TVOC parameter) from modified CBs, while Table 2 lists the detected compounds.

Samples of HCB are characterized by significantly higher values of TVOC parameters than LCB, which can be associated with the higher adsorption capacity of applied CB. It can be seen that obtained TVOC values are about twice as high for HCB as for LCB samples, while their normalization for the WPI content in modified CB samples, which is responsible for VOCs' emissions, points to an even higher difference. Therefore, along with the abovementioned results, it confirms that HCB enables the utilization of significantly higher amounts of WPI material.

Values of TVOC parameters may also be used to identify the environmental impact of analyzed samples. However, their quantitative analysis should be supplemented by the qualitative assessment to determine posed hazards precisely. Table 2 provides details on the detected in gaseous phase VOCs' properties and safety characteristics according to the NFPA 704: Standard System for the Identification of the Hazards of Materials for Emergency Response maintained by the U.S.-based National Fire Protection Association [37] and Globally Harmonized System of Classification and Labelling of Chemicals (GHS) [38]. These international standards describe the impacts of the chemicals on the surrounding environment and human health, as precisely described in previous works [39–41].

For unmodified HCB and LCB samples, various compounds were detected, which may be attributed to their production process, including various purification treatments. For HCB, the most abundant VOCs were 1-propanol and cyclohexane, while for LCB, 1-propanol, 1-methoxy-2-propanol, and 1-ethoxy-2-propanol. Moreover, HCB emitted methylene chloride, while LCB tetrachloroethylene, which are commonly applied as solvents in various industrial processes. According to the recycling company, WPI contained significant amounts of ethanol, ethyl acetate, n-propanol, ethoxypropanol, methoxypropanol, and *n*-propyl acetate, which was mirrored in VOCs emitted from modified CBs. Propanol and its derivatives were the most abundant VOCs detected, accounting even for over 85% of total emissions.

Considering the hazards posed by analyzed samples, it can be seen that most of the detected in gaseous phase VOCs are characterized by relatively low values of flash points and noticeable vapor pressures at ambient temperatures, which classify them as flammable materials.

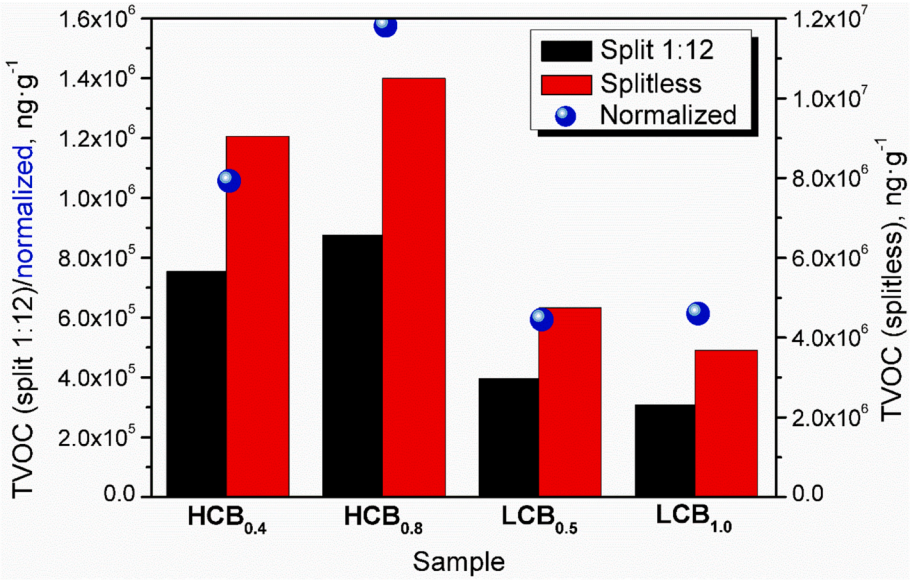

Fig. 2. TVOC emissions determined for the modified CBs with and without the stream splitting on the cold trap, as well as TVOC values normalized for the WPI content in selected samples.

Numerous compounds also show some unfavorable effects on human health, which is expressed by the GHS08: Health Hazard pictogram or score 2 according to NFPA standard (cause temporary incapacitation or a possible residual injury after intense or continued but not chronic exposure). Therefore, proper precautions and process design should be considered when applying WPI materials on an industrial scale. However, considering the application of modified CBs in rubber materials, it is essential that for numerous VOCs, boiling temperature did not exceed 160 °C, which was selected as vulcanization temperature. As presented in the further part of the manuscript, determined vulcanization times for composites containing HCB and LCB were 9.9 and 6.0 min, which should enable efficient evaporation of detected in gaseous phase VOCs. For the application of modified CBs, this time was elongated to 8.4–14.5 min. Therefore, proper ventilation, including a collection of potentially harmful compounds, should be implemented during vulcanization.

3.2. *Properties of rubber composites*

The effect of the CB addition and its type on the curing characteristic at 160 °C and Mooney viscosity at 100 °C of NR is summarized in Table 3. Moreover, Fig. 3 presents plots of samples' curing characteristics, Mooney viscosity, and Mooney viscosity relaxation. It can be seen that while introducing any type of CB resulted in some increase in the minimal torque (M_L), the HCB brought about drastic changes. Such a significant increase in M_L parameter (from 1.1 to 33.4 dNm) indicates more difficult rubber compound processing. This is related to the larger surface area of the HCB compared to the LCB due to the formation of physical bonds of greater intensity [42,43]. On the other hand, the characteristic of rubbers incorporated with WPI-modified CB was intermediate between neat rubber and CB-filled rubbers, which is directly associated with the reduced CB content and the potential migration of WPI components to the rubber phase. It should be noted that M_L values agree with the Mooney viscosity results, which revealed increased viscosity for CB-filled rubbers (including higher for HCB). However, the Mooney viscosity of RHCB could not be determined due to the torque overload occurring already in the initial phase of the measurement. As expected, with the increase in surface area and CB content, the stiffness of the rubber composites increased accordingly, as evidenced by the M_H parameter. Surprisingly, the torque increment (ΔM), which refers to the effectiveness of cure, showed that LCB clearly supports the chemical crosslinking of rubber (ΔM increased almost by 50% compared to the unfilled rubber), in contrast to HCB, which had a negligible effect on this parameter. This proves that there are more functional groups (e.g., sulfur) on the surface of LCB than HCB, allowing for chemical crosslinking with NR in addition to physical bonding [42]. Interestingly, the modification of HCB with WPI led to improved curing efficiency comparable to LCB. This can be explained by the presence of resins or other compounds with reactive groups in the WPI, which could participate in the crosslinking process as well as reduced stiffness of the material, enhancing macromolecular mobility. This might also be the reason for the extension of the optimum cure time for all samples with modified CB (up to 14.5 min for $RHCB_{0.4}$), as well as a reduced cure rate (described by CRI). Therefore, based on the obtained results, it can be assumed that the co-crosslinking of resins contained in WPI, although it improves the effectiveness of rubber curing, requires a longer time to occur. In addition, it is worth mentioning that the aging resistance at 160 °C for all rubber composites was high, which is indicated by low values of the R_{300} parameter (0.3–4.1%), especially for samples filled with WPI-modified CBs.

Table 3 also provides data on samples' density and swelling behavior, described by the swelling degree, sol fraction, and crosslink density. Regardless of the material composition, the density of prepared rubber composites was in the range of 0.94–1.07 g•cm^{-3}. Data on swelling behavior yields somewhat contradictory results for different formulations. Therefore, for further analysis, the values of sol fraction were adopted as the most reliable parameter of the degree of rubber crosslinking, as it does not include the mass of the sample after swelling, which is burdened with a significant error due to the rapid evaporation of toluene. The sol fraction of the rubber slightly decreased after the LCB addition (to 4.1%), while it increased after the HCB addition (to 6.0%), indicating a higher crosslink density of RLCB. These results are consistent with the ΔM parameter, confirming the influence of LCB on the crosslinking efficiency. Moreover, such a phenomenon might be related to the higher adsorption capacity of HCB compared to LCB and the higher content of WPI in the final composite.

The results of the mechanical properties of rubber composites are presented as graphs in Fig. 4. Both the CB surface area and the presence of WPI modification strongly influence the tear strength, tensile properties, rebound resilience, and abrasion resistance of rubber composites. As can be seen in Fig. 4, the incorporation of 30 phr LCB generally significantly improved the mechanical properties of rubber, while the addition of HCB led to their deterioration. These results are consistent

Table 2
Detected representatives of VOCs emitted from as-received and WPI-modified CBs.

Compound	Chemical structure	Formula	NFPA 704			GHS pictograms	Vapor pressure at 25 °C, kPa	Flash point, °C	Boiling point, °C	Sample			
			F	H	I					HCB	$\frac{HCB_{0.4}}{HCB_{0.8}}$	LCB	$\frac{LCB_{0.5}}{LCB_{1.0}}$
Aliphatic hydrocarbons													
Cyclohexane		C_6H_{12}	3	1	0		12.92	-18	80.7	+	- / -	-	- / -
Alcohols													
Ethanol		C_2H_6O	3	2	0		7.91	14	78.2	+	+ / +	+	- / +
Isopropanol		C_3H_8O	3	1	0		6.05	12	82.3	+	- / -	+	- / -
1-Propanol		C_3H_8O	3	1	0		2.80	23	97.2	+	+ / +	+	+ / +
Isobutanol		$C_4H_{10}O$	3	2	0		1.39	28	108.0	-	- / -	-	+ / +
2-Butanol		$C_4H_{10}O$	3	1	0		2.44	24	99.5	-	+ / +	-	- / +
1-Methoxy-2-propanol	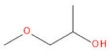	$C_4H_{10}O_2$	3	1	0		1.67	32	120.0	+	+ / +	+	+ / +
1-Ethoxy-2-propanol	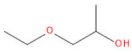	$C_5H_{12}O_2$	2	2	0		1.31	40	133.0	+	+ / +	+	+ / +
Diacetone alcohol	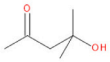	$C_6H_{12}O_2$	2	1	0		0.23	53	167.9	-	- / -	-	+ / +
Propylene glycol		$C_6H_{12}O_2$	1	0	0	-	0.017	99	187.6	-	+ / +	-	+ / +
2-Butoxyethanol	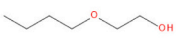	$C_6H_{14}O_2$	2	3	0		0.12	62	168.4	-	+ / +	+	+ / +
Aldehydes													
Octanal	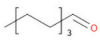	$C_8H_{16}O$	2	0	0		0.16	52	171.0	+	+ / +	+	+ / +
Nonanal	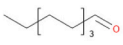	$C_9H_{18}O$	2	2	0		0.049	64	195.0	-	+ / -	+	+ / +
Decanal	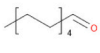	$C_{10}H_{20}O$	2	2	0		0.014	83	212.0	-	+ / -	+	+ / +
Esters													
Ethyl acetate	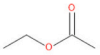	$C_4H_8O_2$	3	1	0		12.43	-4	77.1	-	- / -	+	- / -
n-Propyl acetate	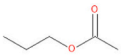	$C_5H_{10}O_2$	3	1	0		4.79	14	101.5	-	+ / +	+	+ / -
1-Methoxy-2-propyl acetate	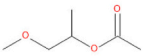	$C_6H_{12}O_3$	2	1	0		0.53	46	145.8	-	+ / +	-	+ / -
Others													
Methylene chloride		CH_2Cl_2	1	2	0		60.00	-	39.8	+	- / -	-	- / -
Tetrachloroethylene		C_2Cl_4	0	2	0		2.47	-	121.2	-	- / -	+	- / -
Acetic acid		$C_2H_4O_2$	2	3	0		2.09	39	117.9	-	+ / +	-	+ / +
Diethyl ether	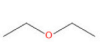	$C_4H_{10}O$	4	1	1		71.73	-45	34.6	-	+ / +	-	- / -

with those reported by Al-Hartomy et al. [44], who found that the addition of low surface area CB (BET surface area of 105 $m^2 \bullet g^{-1}$) improved the tensile strength of NR, but high surface area CB (BET surface area of 1000 $m^2 \bullet g^{-1}$) tended to deteriorate the tensile properties, regardless of the CB content.

The LCB addition increased tear strength from 31.0 to 91.4 $N \bullet mm^{-1}$ and tensile strength from 14.9 to 23.5 MPa and decreased the abrasion from 180 to 135 mm^3 of the neat rubber. On the other hand, the LCB-filled rubber was characterized by slightly reduced elongation at break (−4%) and rebound resilience (−22%) compared to NR, which is typical

Table 3
Curing parameters and Mooney viscosity of prepared NR/CB composites along with their density, swelling degree, sol fraction, and crosslink density.

Property	Sample						
	R0	RHCB	RLCB	$RHCB_{0.4}$	$RHCB_{0.8}$	$RLCB_{0.5}$	$RLCB_{1.0}$
M_L, dNm	1.1	33.4	3.5	4.8	6.7	2.7	2.7
M_H, dNm	22.6	53.0	35.4	34.4	37.4	28.1	27.1
ΔM, dNm	21.5	19.6	31.9	29.6	30.8	25.4	24.4
T_2, min	3.9	2.9	2.8	4.9	4.5	4.7	4.1
T_{90}, min	6.0	9.9	6.0	14.5	13.1	10.0	8.4
CRI, min^{-1}	46.7	14.2	30.9	10.4	11.7	18.8	23.1
R_{300}, %	2.7	1.5	4.1	0.3	0.5	1.5	1.1
MV 100 °C	7.3	–	21.9	24.2	34.3	18.5	19.6
Density, $g{\cdot}cm^{-3}$	0.94 ± 0.01	1.07 ± 0.01	1.05 ± 0.01	1.01 ± 0.01	1.02 ± 0.01	1.02 ± 0.01	1.02 ± 0.01
Swelling degree, %	363 ± 1	239 ± 1	285 ± 2	338 ± 3	332 ± 2	306 ± 3	284 ± 1
Sol fraction, %	4.6 ± 0.1	6.0 ± 0.1	5.0 ± 1.2	6.0 ± 0.3	5.8 ± 0.1	5.3 ± 0.1	4.8 ± 0.2
Crosslink density, $mol{\cdot}cm^{-3}{\cdot}10^{-5}$	6.2 ± 0.1	4.9 ± 0.1	3.8 ± 0.1	2.8 ± 0.1	2.9 ± 0.1	3.4 ± 0.1	4.0 ± 0.1

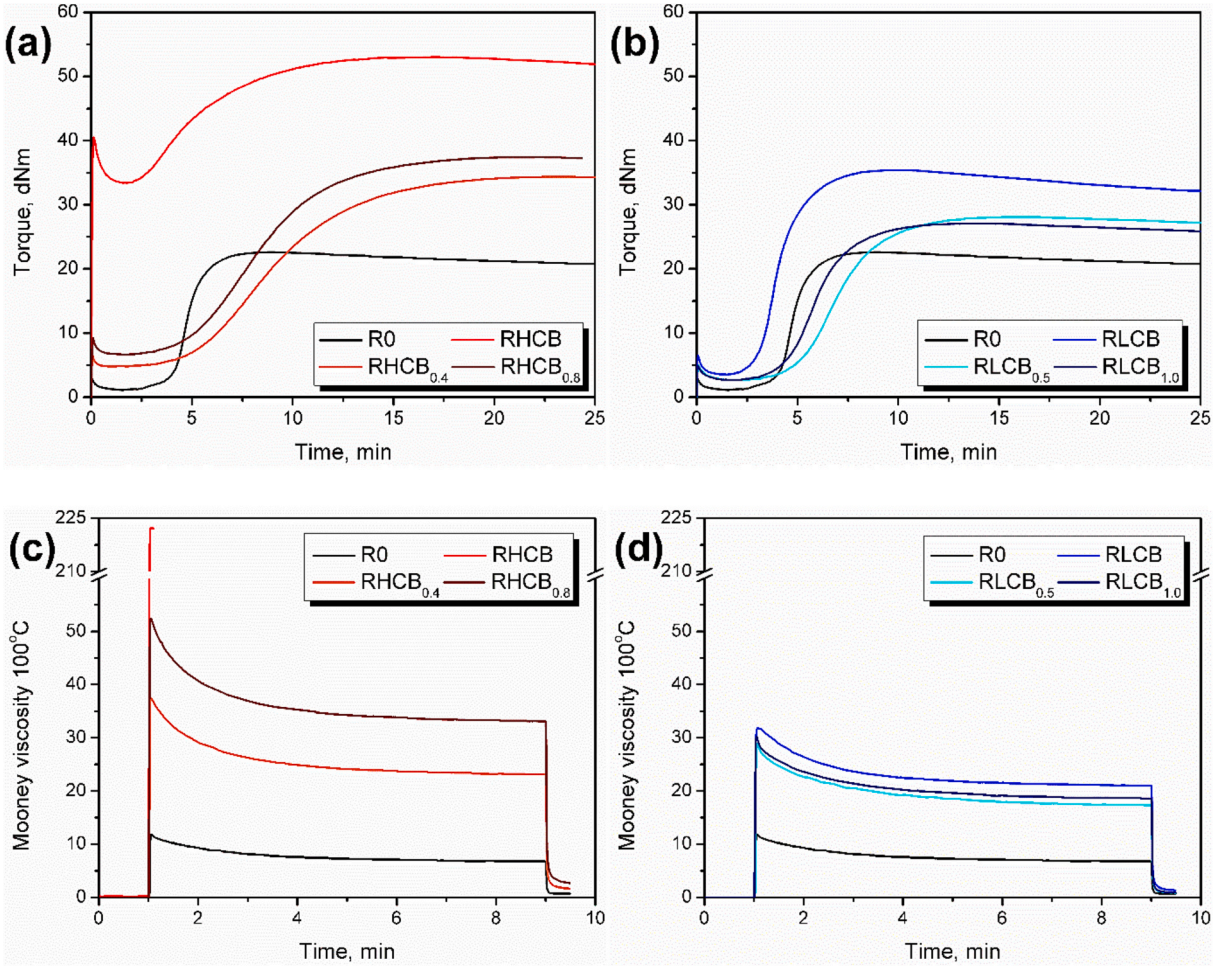

Fig. 3. Plots of (a,b) curing characteristics (at 160 °C), and (c,d) Mooney viscosity for unfilled NR and prepared NR/CB, and NR/CB/WPI composites containing (a,c) HCB and (b,d) LCB.

for compounds with the presence of reinforcing fillers. Interestingly, the LCB modification with WPI further improved the tensile strength to 25.2 MPa, with a WPI:CB ratio of 2:1, and mitigated the damaging effects, leading to a 2% increase in elongation at break and only a 9% decrease in elasticity compared to the reference sample. Nevertheless, the WPI modification of LCB resulted in some deterioration in tear strength and abrasion resistance.

Considering the RHCB system, all investigated mechanical properties were negatively affected by the presence of HCB, with the most significant deterioration noted for elongation at break (by 69%) and rebound resilience (by 65%). Such an effect could be attributed to the high surface area of CB particles, which enhanced the particle-particle interactions and reduced the interfacial adhesion, limiting the stress transfer. However, the HCB modification with WPI resulted in substantial improvement in the properties of the composites, which might be associated with the enhanced mobility of macromolecules due to the potential migration of WPI components to the rubber phase. For example, the $RHCB_{0.4}$ sample achieved an elongation at break of 967% and an elasticity of 53.3%, while the unmodified RHCB sample was 385 and 27.5%, respectively. It should be highlighted that this strategy

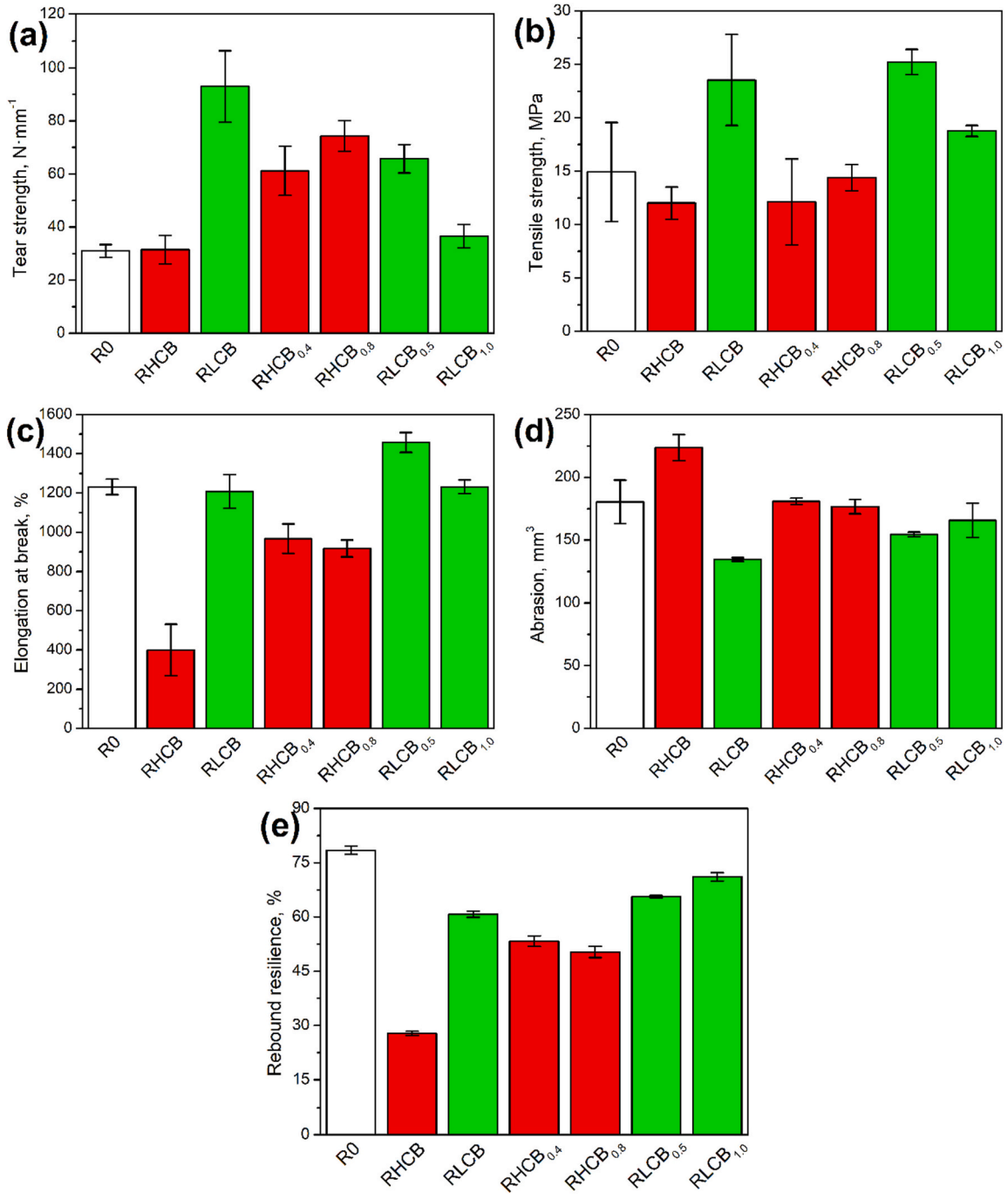

Fig. 4. Graphs visualizing mechanical properties of unfilled NR and NR/CB composites: (a) tear strength, (b) tensile strength, (c) elongation at break, (d) abrasion, (e) rebound resilience, and their changes related to the composition of applied CB.

Table 4
Thermal properties of the studied NR/CB composites determined by various techniques.

Sample	DMA				DSC		TGA		
	E' at 25 °C, MPa	$T_{g\ DMA}$, °C	tan δ at T_g	C_V, %	$T_{g\ DSC}$, °C	ΔC_p, $J \cdot g^{-1} \cdot K^{-1}$	$T_{10\%}$, °C	T_{max}, °C	Residue at 800 °C, %
R0	6.1	−39.6	2.04	–	−56.9	0.383	338	371	2.76
RHCB	77.1	−39.5	0.54	27.3	−59.7	0.222	340	373	25.57
RLCB	12.4	−41.3	1.15	9.5	−58.7	0.269	343	371	24.28
$RHCB_{0.4}$	15.2	−39.7	1.11	10.2	−57.4	0.266	333	371	14.32
$RHCB_{0.8}$	12.7	−42.3	1.00	12.3	−58.7	0.271	338	371	16.84
$RLCB_{0.5}$	7.3	−40.4	1.39	5.9	−57.8	0.302	335	371	14.47
$RLCB_{1.0}$	3.5	−40.2	1.92	0.8	−57.9	0.283	336	372	16.61

increases tear strength by almost 100% compared to neat rubber while maintaining comparable mechanical strength and abrasion resistance.

Thermal properties of rubber composites were assessed based on DMA, DSC, and TGA. The obtained results are summarized in Table 4. DMA measurement provides detailed information about the thermo-mechanical behavior of materials. Plots of storage modulus (E') and loss tangent (tan δ) as a function of temperature are presented in Fig. 5a and b, respectively. A rapid decrease in storage modulus, which results from the energy dissipation within the material, corresponds to the viscoelastic behavior of the rubber associated with its glass transition (α-relaxation). The glass transition temperature (T_g), determined at maximum tan δ, was recorded at approximately −40 °C, regardless of the rubber composition. In addition, it was found that at room temperature, when rubbers are in the elastic state, the stiffness of CB-filled rubbers was higher compared to neat rubber. Expectedly, the highest value of E' (77 MPa) was noted for the RHCB sample, containing CB with a higher surface area, which is in agreement with previous results (M_H parameter).

Except for the stiffness expressed by the E' values, DMA provided important insights in the form of tan δ, which quantifies the materials' ability to dissipate the energy through molecular motions. The decrease in tan δ is associated with the reduced mobility stimulated by the interfacial interactions. According to Bindu and Thomas [45], the extent of these interactions can be quantified using DMA data and expressed as the fraction of polymer chains constrained by the incorporated filler particles following the eqs. (9 and 10):

$$C_v = \frac{(1 - C_0) \bullet \Omega}{\Omega_0} \bullet 100\% \quad (9)$$

$$\Omega = \frac{\pi \bullet tan\delta}{(\pi \bullet tan\delta) + 1} \quad (10)$$

where: C_v – volume fraction of the immobilized polymer chains, %; C_0 – volume fraction of the immobilized chains in pure polymer (taken to be 0), %; Ω and Ω_0 – energy loss fractions for the analyzed sample and pure polymer, respectively.

The values of C_V clearly indicate that the application of WPI as CB modifiers reduces interfacial adhesion, which, however, yields beneficial effects on the composites' mechanical performance. For the incorporation of 30 phr of HCB, over 27% of NR macromolecular chains are efficiently immobilized, which significantly affects the rubbery character.

Notably, the results of T_g determined based on DMA analysis were consistent with the data obtained from DSC measurement. Although the glass transition was detected at a slightly lower value (from −57 to −60 °C), which is typical for different measurement techniques and conditions, it was confirmed that the addition of CB (with and without modification) did not affect the T_g of rubber composites. However, it is worth mentioning that the changes in heat capacity (ΔC_p) related to the glass transition were smaller after the filler was introduced to the system.

Fig. 5c-d shows the TGA (mass loss) and derivative TGA (DTG)

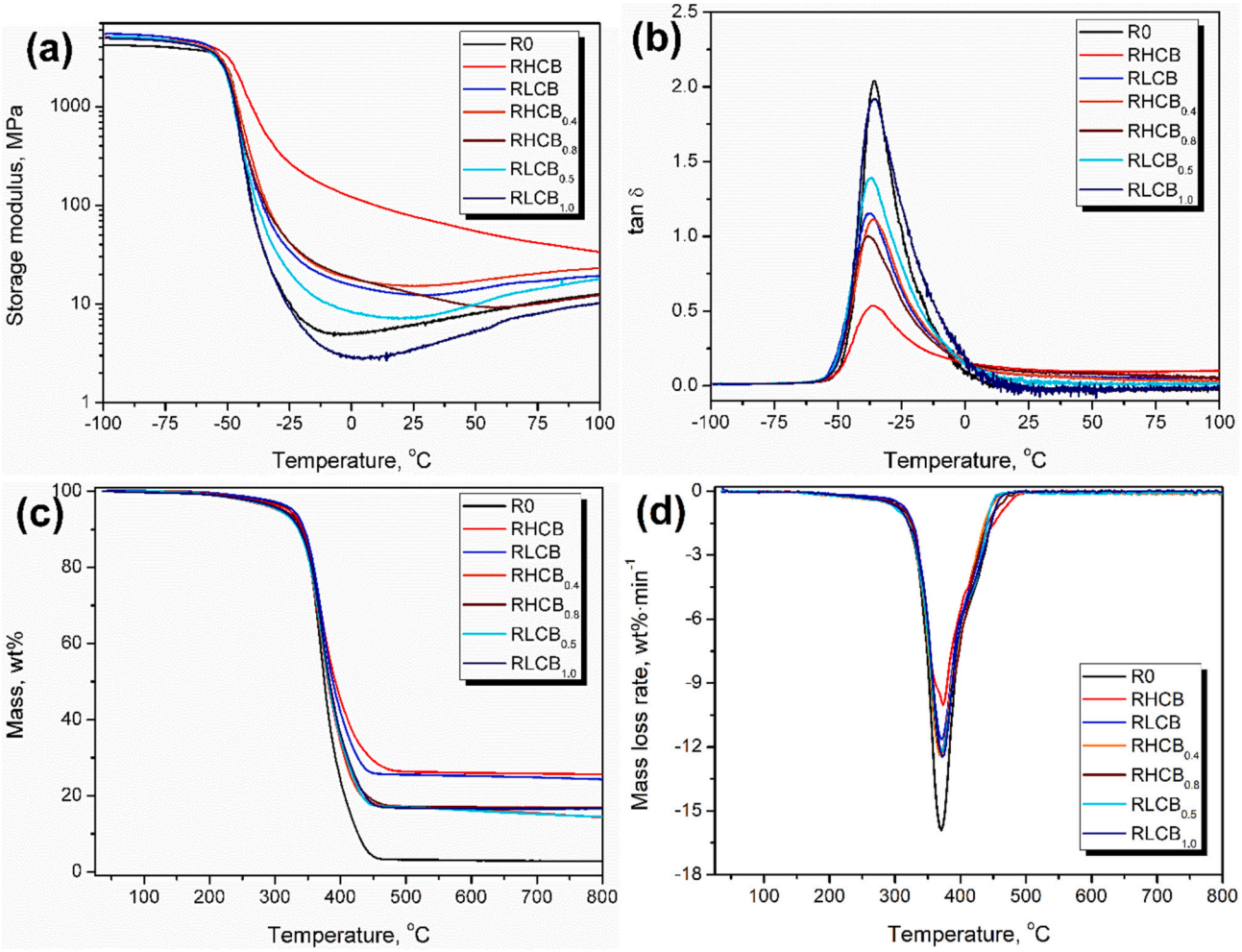

Fig. 5. The results of DMA (a-b) and TGA (c-d) measurements of rubber composites in the form of the temperature dependence of (a) storage modulus, (b) tan δ, (c) mass, and (d) DTG.

curves of the prepared composites. In addition, the temperature at which 10% ($T_{10\%}$) and maximum (T_{max}) weight loss occur and the amount of residual mass are summarized in Table 4. The obtained results indicate that rubber composites undergo a one-stage degradation, which proves the high homogeneity of the systems. The initial decomposition temperature and the maximum degradation temperature were estimated at 340 and 370 °C, respectively, regardless of the material composition. These data are consistent with the literature where the degradation of NR (which is the main component of these composites) occurs at 350–375 °C [46,47]. Although the addition of CB did not affect the thermal stability of the composites, it favored the formation of thermally stable char residue after decomposition, which is promising in terms of fire resistance. It was found that the amount of residue is strictly dependent on the CB content (not type), as it was 24–26% for RHCB and RLCB samples, 14–17% for WPI-modified CB composites, and <3% for unfilled rubber.

4. Conclusions

The presented study proposes a novel strategy for application of WPI as a modifier of CB so as to develop a functional additive to enhance the properties and performance of rubber materials. In view of the reuse of waste materials and seelction of NR as a green elastomer, the resulting composites are of importance from the sustainability standpoint. The results confirmed that the WPI-reinforced CB as the waste material can be efficiently introduced into rubber technology. Proper selection of CB and adjustment of its composition with WPI enables the manufacturing of rubber-based composites with a vast range of properties and performance, including mechanical, thermal, and thermo-mechanical characteristics. Notably, the application of WPI enables one to use less virgin CB during the manufacturing of composites as well as reinforcing rubber materials, providing not only economic but also environmental benefits. The use of high- and low-surface area CB (nominated as HCB and LCB, respectively) ended in different properties and performance of NR composites. First of all, HCB enables one to incorporate higher amounts of WPI into the system. The values of VOC evaluated for as-received and WPI-modified CB additives and composites showed a meaningful difference between VOCs applying various solvents, where HCB and LCB differed obviously. Regarding composite samples, amalgamation of the HCB with WPI led to higher crosslinking efficiency compared to the LCB, notifying additional co-crosslinking of resin in WPI. On teh other hand, mechanical properties were negatively affected by the presence of HCB, such that the highest drop in the elongation at break (-69%) and rebound resilience (-65%) were recorded for HCB-based NR composites. Therefore, it was apparent that domination of particle-particle interactions for HCB-based composites deterioarated the particle-polymer interactions or the interfacial adhesion, which hindered the stress transfer. When modified with WPI, the superiority of HCB to LCB was unraveled. A similalr trend, yet slightly was observed in the case of thermal and thermo-mechanical properties. All in all, the results are promising, but further works should attempt to serve other rubber materials, besides the effects of formulation, curing system, and other carbonaceous additives can be studied. Investigation of flame retardancy and conductivity as two key performance characteristics of the resulting composites, as recently practiced [48], can also useful for exploring the other features of WPI.

Declaration of Competing Interest

The authors declare that they have no known competing financial interests or personal relationships that could have appeared to influence the work reported in this paper.

Data availability

Data will be made available on request.

Acknowledgments

The study was partially co-funded under the project with grants for education allocated by the Ministry of Science and Higher Education in Poland executed under the subject of No 0613/SBAD/4820.

References

[1] Y. Guo, K. Ruan, X. Shi, X. Yang, J. Gu, Factors affecting thermal conductivities of the polymers and polymer composites: a review, Compos. Sci. Technol. 193 (2020), 108134, https://doi.org/10.1016/j.compscitech.2020.108134.
[2] A. Kumar, K. Sharma, A.R. Dixit, A review on the mechanical properties of polymer composites reinforced by carbon nanotubes and graphene, Carbon Lett. 31 (2021) 149–165, https://doi.org/10.1007/s42823-020-00161-x.
[3] H. Vahabi, F. Laoutid, M. Mehrpouya, M.R. Saeb, P. Dubois, Flame retardant polymer materials: an update and the future for 3D printing developments, Mater. Sci. Eng. R. Rep. 144 (2021), 100604, https://doi.org/10.1016/j.mser.2020.100604.
[4] R. Hsissou, R. Seghiri, Z. Benzekri, M. Hilali, M. Rafik, A. Elharfi, Polymer composite materials: a comprehensive review, Compos. Struct. 262 (2021), 113640, https://doi.org/10.1016/j.compstruct.2021.113640.
[5] T. Kuang, J. Ju, T. Liu, A. Hejna, M.R. Saeb, S. Zhang, X. Peng, A facile structural manipulation strategy to prepare ultra-strong, super-tough, and thermally stable polylactide/nucleating agent composites, Adv. Compos. Hybrid. Mater. (2022), https://doi.org/10.1007/s42114-021-00390-2.
[6] N.B. Guerra, G. Sant'Ana Pegorin, M.H. Boratto, N.R. de Barros, C.F. de Oliveira Graeff, R.D. Herculano, Biomedical applications of natural rubber latex from the rubber tree Hevea brasiliensis, Mater. Sci. Eng. C 126 (2021), 112126, https://doi.org/10.1016/j.msec.2021.112126.
[7] M. Sienkiewicz, K. Borzędowska-Labuda, A. Wojtkiewicz, H. Janik, Development of methods improving storage stability of bitumen modified with ground tire rubber: a review, Fuel Process. Technol. 159 (2017) 272–279, https://doi.org/10.1016/j.fuproc.2017.01.049.
[8] R. Wang, J. Zhang, H. Kang, L. Zhang, Design, preparation and properties of bio-based elastomer composites aiming at engineering applications, Compos. Sci. Technol. 133 (2016) 136–156, https://doi.org/10.1016/j.compscitech.2016.07.019.
[9] D. Basu, A. Das, K.W. Stöckelhuber, U. Wagenknecht, G. Heinrich, Advances in layered double hydroxide (LDH)-based elastomer composites, Prog. Polym. Sci. 39 (2014) 594–626, https://doi.org/10.1016/j.progpolymsci.2013.07.011.
[10] L. Bokobza, Multiwall carbon nanotube elastomeric composites: a review, Polymer (Guildf) 48 (2007) 4907–4920, https://doi.org/10.1016/j.polymer.2007.06.046.
[11] K.K. Sadasivuni, D. Ponnamma, S. Thomas, Y. Grohens, Evolution from graphite to graphene elastomer composites, Prog. Polym. Sci. 39 (2014) 749–780, https://doi.org/10.1016/j.progpolymsci.2013.08.003.
[12] Z.A.S. Abdul Salim, A. Hassan, H. Ismail, A review on hybrid fillers in rubber composites, Polym.-Plast. Technol. Eng. 57 (2018) 523–539, https://doi.org/10.1080/03602559.2017.1329432.
[13] S.M.R. Paran, M. Abdorahimi, A. Shekarabi, H.A. Khonakdar, S.H. Jafari, M. R. Saeb, Modeling and analysis of nonlinear elastoplastic behavior of compatibilized polyolefin/polyester/clay nanocomposites with emphasis on interfacial interaction exploration, Compos. Sci. Technol. 154 (2018) 92–103, https://doi.org/10.1016/j.compscitech.2017.11.018.
[14] M.R. Saeb, P. Wiśniewska, A. Susik, Ł. Zedler, H. Vahabi, X. Colom, J. Cañavate, A. Tercjak, K. Formela, GTR/thermoplastics blends: how do interfacial interactions govern processing and Physico-mechanical properties? Materials 15 (2022) 841, https://doi.org/10.3390/ma15030841.
[15] W. Huang, S. Xiao, H. Zhong, M. Yan, X. Yang, Activation of persulfates by carbonaceous materials: a review, Chem. Eng. J. 418 (2021), 129297, https://doi.org/10.1016/j.cej.2021.129297.
[16] P. Wiśniewska, J.T. Haponiuk, X. Colom, M.R. Saeb, Green approaches in rubber recycling technologies: present status and future perspective, ACS Sustain. Chem. Eng. 11 (2023) 8706–8726, https://doi.org/10.1021/acssuschemeng.3c01314.
[17] P. Wiśniewska, A. Hejna, M.R. Saeb, Recycling and processing of waste materials, Materials 16 (2023) 508, https://doi.org/10.3390/ma16020508.
[18] Ł. Zedler, X. Colom, M.R. Saeb, K. Formela, Preparation and characterization of natural rubber composites highly filled with brewers' spent grain/ground tire rubber hybrid reinforcement, Compos. B Eng 145 (2018) 182–188, https://doi.org/10.1016/j.compositesb.2018.03.024.
[19] E. Farida, N. Bukit, E.M. Ginting, B.F. Bukit, The effect of carbon black composition in natural rubber compound, Case Stud. Therm. Eng. 16 (2019), 100566, https://doi.org/10.1016/j.csite.2019.100566.
[20] L. Bokobza, Natural rubber nanocomposites: a review, Nanomaterials 9 (2018) 12, https://doi.org/10.3390/nano9010012.
[21] C.G. Robertson, N.J. Hardman, Nature of carbon black reinforcement of rubber: perspective on the original polymer nanocomposite, Polymers (Basel) 13 (2021) 538, https://doi.org/10.3390/polym13040538.
[22] J. Song, K. Tian, L. Ma, W. Li, S. Yao, The effect of carbon black morphology to the thermal conductivity of natural rubber composites, Int. J. Heat Mass Transf. 137 (2019) 184–191, https://doi.org/10.1016/j.ijheatmasstransfer.2019.03.078.
[23] S. Salaeh, C. Nakason, Influence of modified natural rubber and structure of carbon black on properties of natural rubber compounds, Polym. Compos. 33 (2012) 489–500, https://doi.org/10.1002/pc.22169.

[24] M. Dominic, R. Joseph, P.M. Sabura Begum, B.P. Kanoth, J. Chandra, S. Thomas, Green tire technology: effect of rice husk derived nanocellulose (RHNC) in replacing carbon black (CB) in natural rubber (NR) compounding, Carbohydr. Polym. 230 (2020), 115620, https://doi.org/10.1016/j.carbpol.2019.115620.
[25] M. Li, L. Zhu, H. Xiao, T. Shen, Z. Tan, W. Zhuang, Y. Xi, X. Ji, C. Zhu, H. Ying, Design of a Lignin-Based Versatile Bioreinforcement for high-performance natural rubber composites, ACS Sustain. Chem. Eng. 10 (2022) 8031–8042, https://doi.org/10.1021/acssuschemeng.2c02113.
[26] D. Saini, R. Aggarwal, S.R. Anand, N. Satrawala, R.K. Joshi, S.K. Sonkar, Sustainable feasibility of waste printer ink to magnetically separable iron oxide–doped nanocarbons for styrene oxidation, Mater. Today Chem. 16 (2020), 100256, https://doi.org/10.1016/j.mtchem.2020.100256.
[27] D. Saini, R. Aggarwal, S.R. Anand, S.K. Sonkar, Sunlight induced photodegradation of toxic azo dye by self-doped iron oxide nano-carbon from waste printer ink, Sol. Energy 193 (2019) 65–73, https://doi.org/10.1016/j.solener.2019.09.022.
[28] M. Parthasarathy, Challenges and emerging trends in toner waste recycling: a review, Recycling 6 (2021) 57, https://doi.org/10.3390/recycling6030057.
[29] C. Reichardt, Solvents and Solvent Effects in Organic Chemistry, Wiley, 2002, https://doi.org/10.1002/3527601791.
[30] M. Marć, J. Namieśnik, B. Zabiegała, The miniaturised emission chamber system and home-made passive flux sampler studies of monoaromatic hydrocarbons emissions from selected commercially-available floor coverings, Build. Environ. 123 (2017) 1–13, https://doi.org/10.1016/j.buildenv.2017.06.035.
[31] M. Marć, B. Zabiegała, An investigation of selected monoaromatic hydrocarbons released from the surface of polystyrene lids used in coffee-to-go cups, Microchem. J. 133 (2017) 496–505, https://doi.org/10.1016/j.microc.2017.04.015.
[32] E. Massold, C. Bähr, T. Salthammer, S.K. Brown, Determination of VOC and TVOC in air using thermal desorption GC-MS – practical implications for test chamber experiments, Chromatographia 62 (2005) 75–85, https://doi.org/10.1365/s10337-005-0582-z.
[33] T.H. Khang, Z.M. Ariff, Vulcanization kinetics study of natural rubber compounds having different formulation variables, J. Therm. Anal. Calorim. 109 (2012) 1545–1553, https://doi.org/10.1007/s10973-011-1937-3.
[34] P.J. Flory, J. Rehner, Statistical mechanics of cross-linked polymer networks I. Rubberlike elasticity, J. Chem. Phys. 11 (1943) 512–520, https://doi.org/10.1063/1.1723791.
[35] G. Kraus, Swelling of filler-reinforced vulcanizates, J. Appl. Polym. Sci. 7 (1963) 861–871, https://doi.org/10.1002/app.1963.070070306.
[36] P. Garrido, F. Concha, R. Bürger, Settling velocities of particulate systems: 14. Unified model of sedimentation, centrifugation and filtration of flocculated suspensions, Int. J. Miner. Process. 72 (2003) 57–74, https://doi.org/10.1016/S0301-7516(03)00087-5.
[37] National Fire Protection Association, NFPA 704: A Standard System for the Identification of the Hazards of Materials for Emergency Response [WWW Document]. https://www.nfpa.org/codes-and-standards/all-codes-and-standards/list-of-codes-and-standards/detail?code=704, 2022.
[38] European Parliament and the Council, Regulation (EC) No 1272/2008 of the European Parliament and of the Council of 16 December 2008 on Classification, labelling and Packaging of Substances and Mixtures, Amending and Repealing directives 67/548/EEC and 1999/45/EC, and Amending Regulation (EC) No 1907/2006. https://eur-lex.europa.eu/LexUriServ/LexUriServ.do?uri=OJ:L:2008:353:0001:1355:EN:PDF, 2008.
[39] A. Hejna, M. Marć, J. Korol, Modification of cellulosic filler with diisocyanates – volatile organic compounds emission assessment and stability of chemical structure over time, Nord. Pulp Paper Res. J. 36 (2021) 353–372, https://doi.org/10.1515/npprj-2020-0104.
[40] A. Hejna, M. Marć, D. Kowalkowska-Zedler, A. Pladzyk, M. Barczewski, Insights into the thermo-mechanical treatment of brewers' spent grain as a potential filler for polymer composites, Polymers (Basel) 13 (2021), https://doi.org/10.3390/polym13060879.
[41] A. Hejna, M. Marć, K. Skórczewska, J. Szulc, J. Korol, K. Formela, Insights into modification of lignocellulosic fillers with isophorone diisocyanate: structure, thermal stability and volatile organic compounds emission assessment, Eur. J. Wood and Wood Product. 79 (2021) 75–90, https://doi.org/10.1007/s00107-020-01604-y.
[42] Z.H. Li, J. Zhang, S.J. Chen, Effects of carbon blacks with various structures on vulcanization and reinforcement of filled ethylene-propylene-diene rubber, Express Polym Lett 2 (2008) 695–704, https://doi.org/10.3144/expresspolymlett.2008.83.
[43] P. Noorunnisa Khanam, M.A. AlMaadeed, M. Ouederni, B. Mayoral, A. Hamilton, D. Sun, Effect of two types of graphene nanoplatelets on the physico–mechanical properties of linear low–density polyethylene composites, Adv. Manuf.: Polym. & Composit. Sci. 2 (2016) 67–73, https://doi.org/10.1080/20550340.2016.1235768.
[44] O.A. Al-Hartomy, F. Al-Solamy, A. Al-Ghamdi, N. Dishovsky, M. Ivanov, M. Mihaylov, F. El-Tantawy, Influence of carbon black structure and specific surface area on the mechanical and dielectric properties of filled rubber composites, Int. J. Polym. Sci. 2011 (2011) 1–8, https://doi.org/10.1155/2011/521985.
[45] P. Bindu, S. Thomas, Viscoelastic behavior and reinforcement mechanism in rubber nanocomposites in the vicinity of spherical nanoparticles, J. Phys. Chem. B 117 (2013) 12632–12648, https://doi.org/10.1021/jp4039489.
[46] M.J. Fernández-Berridi, N. González, A. Mugica, C. Bernicot, Pyrolysis-FTIR and TGA techniques as tools in the characterization of blends of natural rubber and SBR, Thermochim. Acta 444 (2006) 65–70, https://doi.org/10.1016/j.tca.2006.02.027.
[47] S. Rooj, A. Das, V. Thakur, R.N. Mahaling, A.K. Bhowmick, G. Heinrich, Preparation and properties of natural nanocomposites based on natural rubber and naturally occurring halloysite nanotubes, Mater. Des. 31 (2010) 2151–2156, https://doi.org/10.1016/j.matdes.2009.11.009.
[48] P. Wiśniewska, N.A. Wójcik, J. Ryl, R. Bogdanowicz, H. Vahabi, K. Formela, M. R. Saeb, Rubber wastes recycling for developing advanced polymer composites: A warm handshake with sustainability, J. Clean. Prod. 427 (2023) 139010, https://doi.org/10.1016/j.jclepro.2023.139010.